Pergamon

PII: S0038-092X(97)00022-4

Solar Energy Vol. 60, No. 6, pp. 333–346, 1997

0038-092X/97 $17.00+0.00

NUMERICAL SIMULATION OF SOIL HEAT EXCHANGER-STORAGE SYSTEMS FOR GREENHOUSES

CAROL GAUTHIER, * MARCEL LACROIX *† and HERVÉ BERNIER **
* Groupe Thermaus, Faculté des Sciences Appliquées, Université de Sherbrooke, Sherbrooke, Québec, J1K 2R1, Canada and ** Institut de technologie agro-alimentaire, La Pocatière, Québec, G0R 1Z0, Canada

Received 27 August 1996; revised version accepted 27 February 1997

Communicated by J. OWEN LEWIS

Abstract—A numerical study was conducted for the thermal behavior of soil heat exchanger-storage systems (SHESSs) aimed at reducing the energy consumption of greenhouses. These systems consist of buried pipes circulating air for storing and removing heat from the soil. First, a transient fully three-dimensional heat transfer model resting on the coupled conservation equations of energy for the soil and the circulating air is presented. The model is validated with experimental data taken from a SHESS installed in a commercial type greenhouse. Next, the model is used to examine the effect of various design and operating parameters on the performance of SHESSs. Results indicate that the total amount of energy stored or recovered daily per volume Q_v decreases exponentially with the pipe center-to-center distance and the pipe length. It increases with the air velocity and this effect is enhanced as the pipe center-to-center distance diminishes. Nevertheless, as a compromise between cost and performance, it appears that an air blowing velocity of 4 m s^{-1} is nearly optimal. As the moisture content of the soil increases, Q_v augments but its effect becomes negligible for large pipe lengths and small blowing velocities. Adding side insulation improves the performance of the SHESS but the beneficial effect of insulation underneath the bottom pipe row is significant. Finally, burying pipes deeper underground allows more energy to be stored during the day but less is recovered at night through the ground surface and the overall performance declines. © 1997 Elsevier Science Ltd.

1. INTRODUCTION

Commercial greenhouses have, in general, a low thermal mass. Excess solar heat captured during the day is ventilated to the outside, while auxiliary heat must be supplied at night in order to maintain proper indoor conditions. Although increasing the thermal mass using water tanks, crushed stones or phase-change materials provides reduction in energy requirements, the high capital costs involved in obtaining and/or containing these materials have limited their use. In contrast, the soil beneath a greenhouse has a significant thermal mass which is readily available and inexpensive. To exploit effectively the heat storage capacity of the soil, a heat exchanger-storage system as shown in Fig. 1 was devised. This system is made of an array of buried pipes running along the length of the greenhouse with their inlets and outlets at opposing ends. During sunny days, the excess heat in the air is transferred from inside the greenhouse, through the pipes, to the ground. At night, the stored heat is recovered by circulating cold air from the greenhouse through the pipes. The air is collected at the top of the greenhouse during the day and at ground level during the night to increase the rate of heat exchange.

Over the last two decades, SHESSs have been installed in a variety of greenhouses. Santamouris *et al.* (1994) give an overview of several successful experiments. Although these applications can provide some indications on the design and operating conditions of these systems, they cannot, however, be generalized for every greenhouses. To optimize the design and operating condition of a SHESS for a given greenhouse, a flexible and accurate computational tool is required. For this reason, a number of authors have proposed different models for the prediction of the thermal behavior of SHESSs with buried pipes. The early models are one-dimensional single pipe models (Santamouris and Lefas, 1986; Rodriguez *et al.*, 1988). They do not calculate the heat transfer in the soil. Two-dimensional models have also been developed. For instance, Schiller (1982) reported on a axisymmetric model for a single pipe with heat conduction around the pipe and temperature dependent soil thermal properties. Mihalakakou *et al.* (1994a) proposed a transient axisymmetric model for a single pipe which takes into account the temperature gradients prevailing beneath the ground surface. The tem-

†Author to whom correspondence should be addressed.

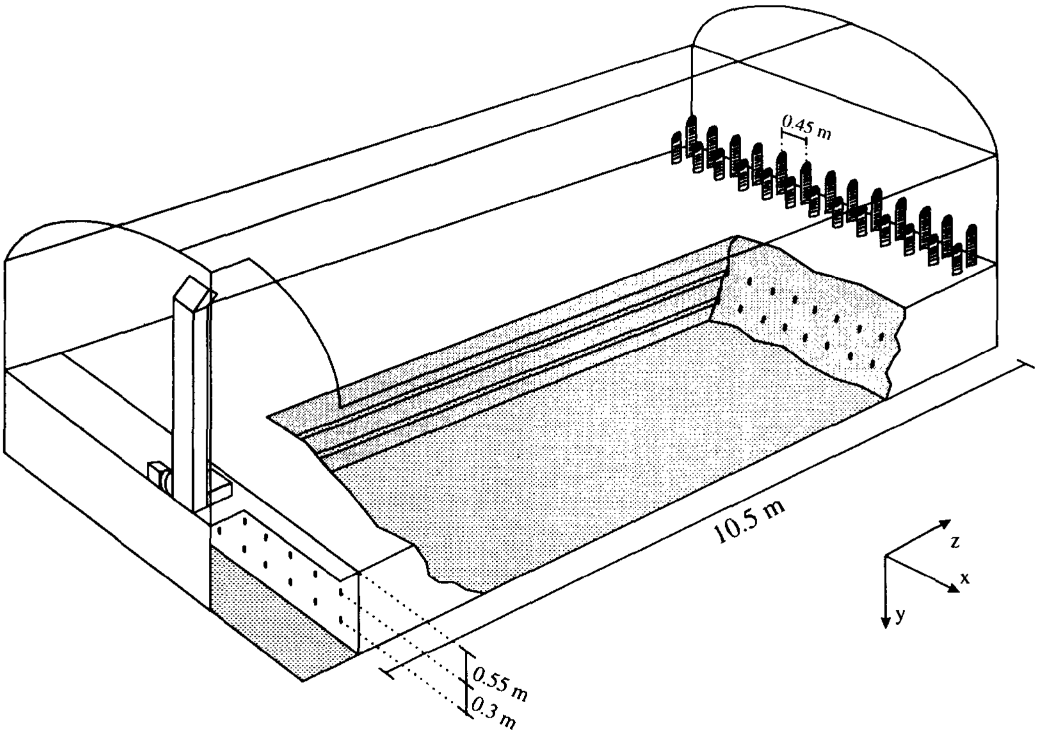

Fig. 1. Soil heat exchanger-storage system.

perature of the soil in the vicinity of the pipe is estimated by superposing the temperature field caused by the pipe system to the unperturbed temperature field caused by the ground surface temperature. The model is also capable of predicting the soil moisture content as well as the humidity of the circulating air. The model was later extended for several parallel pipes using the method of superposition (Mihalakakou *et al.*, 1994b). Sawhney and Mahajan (1994) and Sodha *et al.* (1994) proposed analytical models to determine the annual heating and cooling potential of underground air pipe systems. Both models assume constant and homogeneous thermal properties of the soil and ignore condensation and evaporation within the pipes. Moreover, the Sodha *et al.* model neglects the hourly variations of the input time-dependent parameters (ambient air temperature, solar radiation, relative humidity).

More recently, Mihalakakou *et al.* (1995) reported on a three-dimensional model for the prediction of the ground temperature at various depths below buildings. The authors claim that their model can also be used to determine the ground temperature profile when an earth-to-air heat exchanger system is buried under the building. In this case however, the ground temperature at a certain point in the vicinity of the pipe is estimated by the superposition of the soil temperature caused by the presence of the heat exchanger and of the soil temperature caused by the ground surface boundary.

None of the aforementioned models is capable of directly predicting the fully transient three-dimensional heat transfer in a multiple-pipe SHESS. Moreover, concrete foundations and their insulation, which play a significant role in the overall heat transfer process, were ignored. As a result, the use of these simplified models for the design of SHESSs is limited and may hardly yield an optimized solution in most practical situations.

The present article describes a model that alleviates the drawbacks mentioned in the previous paragraph. A fully transient three-dimensional heat transfer model is presented for SHESSs. The model may handle multiple buried pipes, non-homogeneous soil properties, concrete foundations and insulation, transient boundary conditions and condensation and evaporation in the pipes. The model is thoroughly validated with experimental data taken from a soil heat exchanger storage system installed in a commercial-type greenhouse. It is next employed to conduct a parametric study on the design and operation of SHESSs for greenhouses.

2. PHYSICAL MODEL AND NUMERICAL PROCEDURE

The physical model of the SHESS is illustrated schematically in Fig. 1. This system was described in the previous section. The heat transfer model is based on the following assumptions.

(1) Conduction heat transfer is transient and fully three-dimensional in the soil.
(2) The thermophysical properties of the soil are constant, and temperature independent but may be non-homogeneous.
(3) Heat transfer caused by moisture gradients in the soil is negligible with respect to that by temperature gradients.
(4) Heat transfer in the pipes is dominated by convection in the axial direction. It is, however, coupled with the temperature field in the soil via the boundary condition on the pipes surface.
(5) Condensation and evaporation in the pipes are taken into account.
(6) Pipes of circular cross-section are modelled as pipes of square cross-section of equivalent areas.

Assumption (3) is justified by the fact that the heat transfer processes (charge and discharge of the soil) take place over periods of 24 h and involve temperature differences of less than 10 K. As a result, a dimensional analysis conducted by Gauthier (1994) has revealed that even for extreme cases, the moisture gradients account for less than 0.1% of the total heat transfer in the soil. Puri (1986) also reached the conclusion that the moisture movements has little effect on the heat transfer in the soil because the thermal diffusivity of the soil shows little variation with water content. The thermal conductivity increases with water content but so does, in a similar proportion, the volumetric heat capacity.

Assumption (6) was adopted so that a simple cartesian coordinate system could be used. This assumption considerably simplifies the numerical model without sacrificing accuracy in the numerical predictions. Moreover, to correctly calculate the amount of heat transferred from the pipe to the ground, the convective heat transfer coefficient for a square pipe is set equal to the actual heat transfer coefficient multiplied by a factor of $\sqrt{\pi}/2$. This factor represents the ratio of the perimeter of a circle to that of a square of equal area.

Subjected to the foregoing assumptions, the governing equations for the conservation of energy may be stated as;

$$C\frac{\partial T}{\partial t}=\frac{\partial}{\partial x}\left(k\frac{\partial T}{\partial x}\right)+\frac{\partial}{\partial y}\left(k\frac{\partial T}{\partial y}\right)+\frac{\partial}{\partial z}\left(k\frac{\partial T}{\partial z}\right)+S, \tag{1}$$

for the soil, the concrete and the insulation, and

$$\frac{\mathrm{d}H}{\mathrm{d}z}=\frac{q'}{VA_s}-\frac{\mathrm{d}\omega}{\mathrm{d}z}\rho h_L \tag{2}$$

for the pipes.

The second term on the right hand side of eqn (2) takes into account the variation of the moisture content of the air as it flows along the pipe (condensation or evaporation).

The volumetric heat capacity C and the thermal conductivity k in eqn (1) are expressed in terms of the soil moisture content as;

$$C=C_{\mathrm{Cte}}+C_\theta\theta \tag{3}$$

$$k=k_{\mathrm{Cte}}+k_\theta\theta \tag{4}$$

The parameters C_{cte}, C_θ, k_{Cte} and k_θ are determined using the de Vries (1975) relations for the moist soil. C_θ and k_θ are set to zero for all other components like concrete and insulation.

The boundary conditions for the above conservation equations are as follows. At the pipe inlet

$$H(0)=H_{\mathrm{in}} \tag{5}$$

where H_{in} is provided by experimental data.

The underground lateral external surfaces of the computational domain are assumed to be adiabatic, i.e.

$$\frac{\partial T}{\partial n}=0 \tag{6}$$

where n is a unit vector normal to the surface.

A constant and uniform temperature for the horizontal plane deep underground is imposed. At the ground surface;

$$k_{\mathrm{soil}}\frac{\partial T_{\mathrm{soil}}}{\partial y}=h(T_{\mathrm{soil}}-T_{\mathrm{surr}}) \tag{7}$$

where T_{surr} is the temperature of the surroundings and h is the heat transfer coefficient estimated with an empirical correlation. Finally, eqns (1) and (2) are coupled via the heat flux q' given by the boundary condition at the pipe surface, i.e.;

$$q'=Ph_c(T_{\mathrm{soil}}-T_{\mathrm{air}}) \tag{8}$$

The finite difference equations are obtained by integrating eqn (1) over each control volumes in the x, y, z space and eqn (2) in the z direction for each pipe. (Figs 2 and 3). The resulting finite difference scheme has the form:

$$a_P T_P = a_W T_W + a_E T_E + a_S T_S + a_N T_N + a_B T_B + a_T T_T + b_P \quad (9)$$

$$H_T = H_B + \frac{q_P}{VA_S} + (\omega_B - \omega_T)\rho h_L \quad (10)$$

where

$$a_W = 2\delta y_P \delta z_P \left[\frac{\delta x_W}{k_W} + \frac{\delta x_P}{k_P}\right]^{-1}$$

$$a_E = 2\delta y_P \delta z_P \left[\frac{\delta x_E}{k_E} + \frac{\delta x_P}{k_P}\right]^{-1}$$

$$a_S = 2\delta x_P \delta z_P \left[\frac{\delta y_S}{k_S} + \frac{\delta y_P}{k_P}\right]^{-1}$$

$$a_N = 2\delta x_P \delta z_P \left[\frac{\delta y_N}{k_N} + \frac{\delta y_P}{k_P}\right]^{-1} \quad (11)$$

$$a_B = 2\delta x_P \delta y_P \left[\frac{\delta z_B}{k_B} + \frac{\delta z_P}{k_P}\right]^{-1}$$

$$a_T = 2\delta x_P \delta y_P \left[\frac{\delta z_T}{k_T} + \frac{\delta z_P}{k_P}\right]^{-1}$$

$$a_P = C_p \frac{\delta V_P}{\delta t} + a_W + a_E + a_S + a_N + a_B + a_T - St_P \delta V_P \quad (12)$$

$$b_P = \delta V_P \left(Sc_P + \frac{C_P}{\delta t} T_P^0\right) \quad (13)$$

Equations (9) and (10) are solved iteratively at each time step until convergence. Convergence is declared when the maximum local temperature change over the entire domain and between two consecutive iterations is less than a preset value of 0.001 K. The condensation and evaporation rates along each pipe are also calculated in the iterative process. Further, in order to verify the numerical solution obtained, the present calculation procedure keeps track of the overall energy balance; at any time, the change in internal energy of the system must be equal to the total energy supplied or extracted at all boundaries, including the surface of the buried pipes.

3. VALIDATION AND EXPERIMENTS

The foregoing model was first validated by comparing thoroughly its numerical predictions with the analytical solutions for one, two and three-dimensional conduction heat transfer problems subjected to Dirichlet, Neumann and mixed boundary conditions. Its transient predictions were also compared with that of the well known but more elaborate and time consuming commercial software FLOW3D (AEA, 1992).

Next the model was validated with experimental data taken from a SHESS installed in a commercial-type greenhouse located in La Pocatière, Québec, CANADA (Bernier *et al.*, 1990a; Bernier *et al.*, 1990b). A schematic representation of the system is shown in Fig. 1. The greenhouse has a surface area of $12.1 \times 6.5\ m^2$ and lies on a 1.4 m high concrete foundation insulated on the inside with 76 mm thick polystyrene panels. The greenhouse is covered by

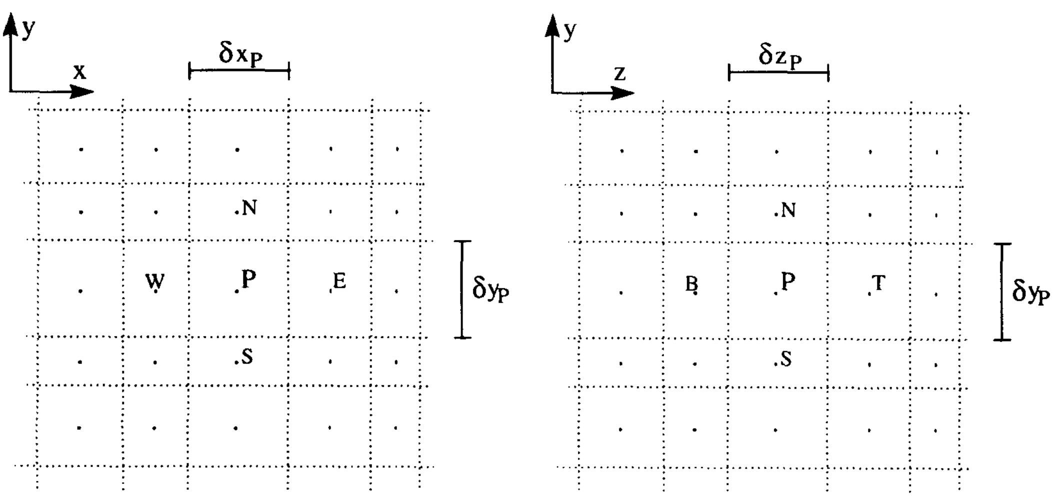

Fig. 2. xy-plane representation of the control volume discretization within the soil.

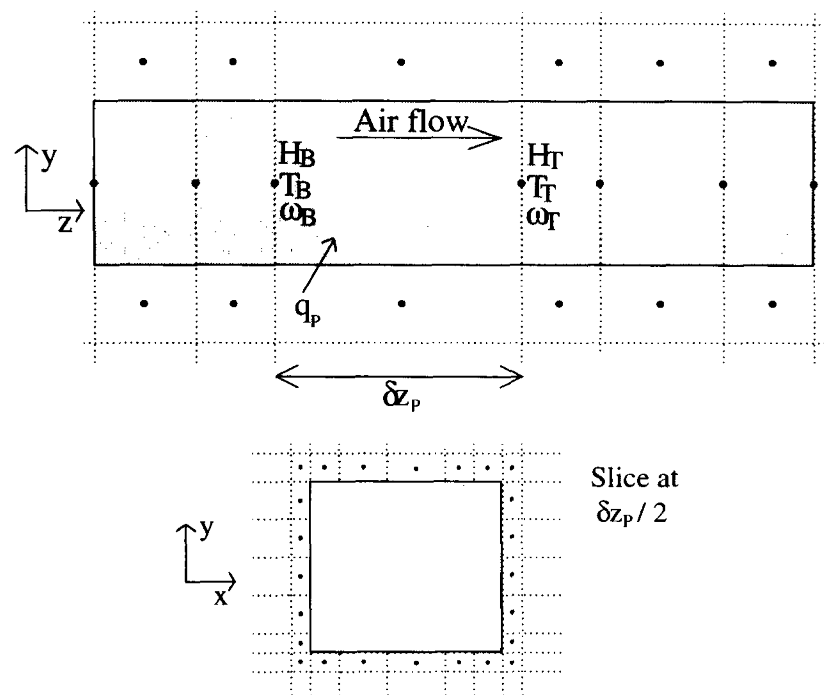

Fig. 3. Control volume discretization of a pipe within the soil.

hollow profile double skin polycarbonate panels 6 mm thick and its north wall is insulated. It is equipped with a thermal curtain in order to diminish the heat losses during the night. It is also equipped with an artificial lighting system and a standard heating and ventilation equipment. The period of experimentation ran from September 1985 to September 1987. Three consecutive days of experimentation have been chosen to validate the model, that is, from April 22 to April 25 1986. These typical days correspond to a period of the year for which the system is expected to perform with the highest efficiency. In the spring, the moisture content of the soil reaches a maximum thereby favoring its conductivity and heat capacity. Further, at this time of the year, overheating occurs during the day while the heating load is still high during the night.

The heat exchanger-storage system is made of 26 non-perforated, corrugated plastic drainage pipes, 102 mm in diameter (inside) buried in the soil. Two rows of 13 pipes, 10.5 m long, are buried at 450 mm and 750 mm depths, respectively. The pipes are parallell to the longitudinal axis of the greenhouse and are spaced 450 mm apart. A 0.75 kW blower circulates air, collected in the greenhouse, through the pipes at a total flowrate of 0.91 $m^3 s^{-1}$. This volumetric flowrate yields an average air velocity of 3.8 $m s^{-1}$ in each pipe. Its daily energy consumption was estimated at 6.5×10^7 joules. The blower has its air intake above the thermal curtain near the ridge for daytime operation, and below the curtain near the soil surface, for night operation. The air is discharged into the greenhouse from the 26 pipe outlets that emerge from the soil. The total cost of the system and its installation was estimated at \$1340 (1986 Canadian dollars), \$440 dollars having been spent on the buried pipes.

As a result of the periodic symmetry of the heat flow patterns observed in the soil, only 12 of the 26 pipes included in the SHESS are modelled (Fig. 4). The validation have been performed using three different grid sizes consisting of $125 \times 50 \times 10$ (grid 1), $179 \times 77 \times 10$ (grid 2) and $275 \times 111 \times 10$ (grid 3) nonuniformly distributed control volumes in the x, y and z directions respectively. A uniform temperature of 281.15 K was maintained at a depth of 3.09 m in the soil. This boundary condition takes into account the energy drained by the seeping water below the water table which sits at approximately 3 m below the ground surface. A convective heat transfer coefficient of 5 $W m^{-2} K^{-1}$ was imposed on the floor inside the greenhouse while a coefficient of 10 $W m^{-2} K^{-1}$ was set at the ground surface outside.

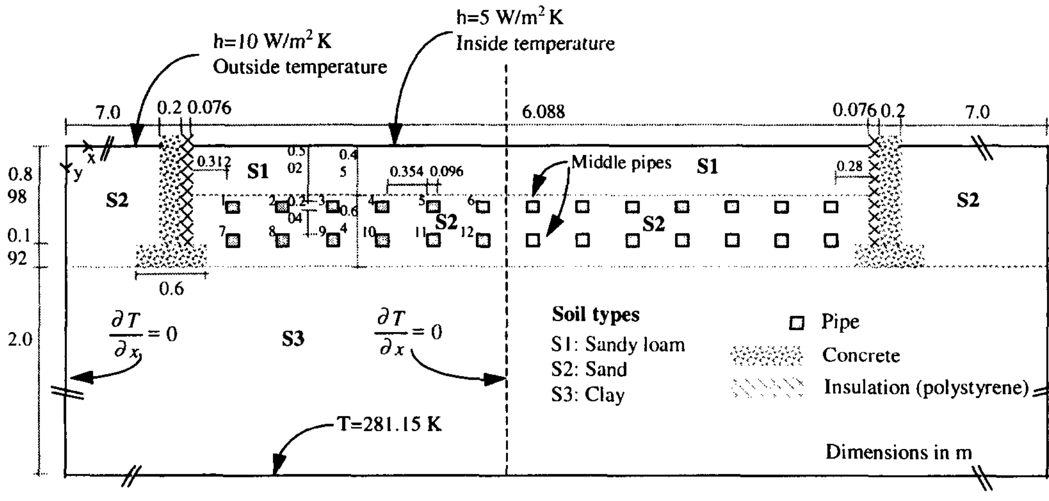

Fig. 4. Model representation of the soil heat exchanger-storage system in the xy-plane.

The temperatures inside and outside the greenhouse were taken from experimental measurements and are shown in Fig. 5 along with the measured pipe inlet air temperatures. The measured pipe inlet humidities were also used as inputs in the model (Fig. 6). The convective heat transfer coefficient h_c for the air flow inside corrugated pipes was estimated at 23 W m^{-2} K^{-1} using the correlation of Sibley and Raghavan (1984). The outermost vertical boundaries of the domain were considered adiabatic. Finally, the nonhomogeneous thermophysical properties of the soil were determined with de Vries's relation (de Vries, 1975). They are summarized in Table 1.

Figures 7 and 8 display the predicted and measured temporal variation of the temperature difference between the inlet and the outlet of pipes nos 6 and 12 for three consecutive days

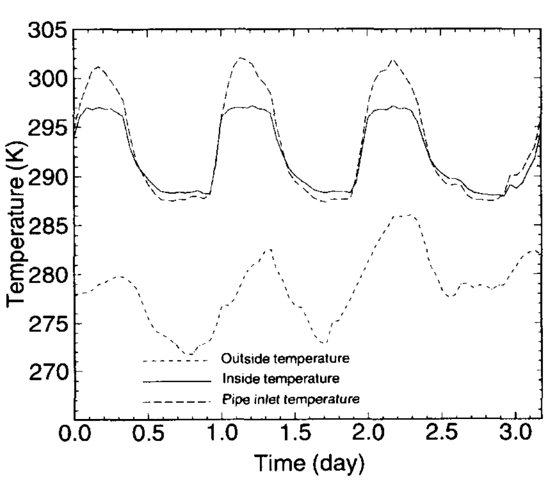

Fig. 5. Inlet temperatures for the model validation.

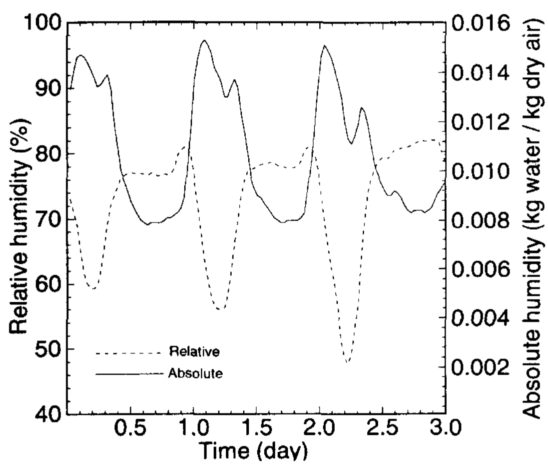

Fig. 6. Inlet humitidies for the model validation.

respectively. The authors feel that the temperature difference is more representative (and challenging) of the model predictive capabilities and accuracy than the outlet temperature alone which is usually displayed in other studies (Mihalakakou et al., 1994a,b; Tzaferis et al., 1992). The predicted results are given for the three grid sizes in each figure. For pipe no. 6 (Fig. 7), the results exhibit a maximum relative discrepancy of 5.2% between the predictions and the experimental data with the coarest grid (grid 1). This discrepancy diminishes to 4.2% when the finest grid is employed (grid 3). The results for pipe no. 12 (Fig. 8), show, on the other hand, that the maximum relative discrepancies for the coarsest and the finest grids are 3% and 2% respectively. The larger error observed for pipe no. 6 is most likely caused by an over-estimation of the heat transfer coeffi-

Table 1. Properties of the soil and of the greenhouse underground components

	Porosity	θ	k (W m^{-1} K^{-1})	C (J m^{-3} K^{-1})
Soil type S1	0.6	0.2 to 0.4	0.98 to 1.2	1.66×10^6 to 2.50×10^6
Soil type S2	0.45	0.4	2.4	2.94×10^6
Soil type S3	0.45	0.45	2.55	3.15×10^6
Concrete	–	–	0.72	1.45×10^6
Insulation	–	–	0.027	6.65×10^4

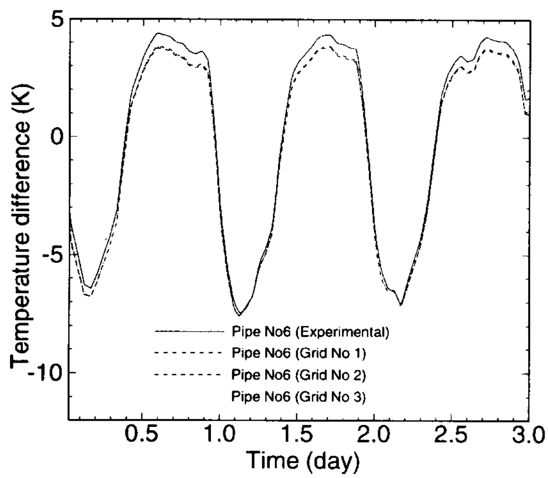

Fig. 7. Predicted and measured inlet/outlet temperature differences for pipe no. 6.

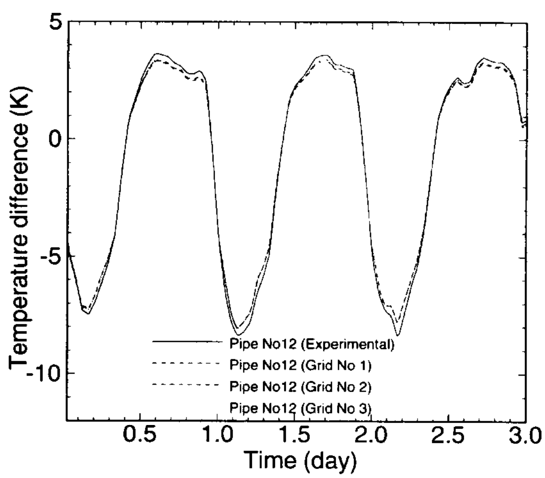

Fig. 8. Predicted and measured inlet/outlet temperature differences for pipe no. 12.

cient at the ground surface and of the soil thermal diffusivity in region S1. Nonetheless, the agreement between the simulation and the experiment is remarkable considering the fact that the soil thermophysical properties, which strongly influence the thermal behavior of the system, can hardly be estimated within an accuracy of $\pm 10\%$ and that these properties are subjected to seasonal changes. Further, the minor gain in precision brought by the refinement of the grid sizes is not worthwhile considering the substantial increase in the simulation time (6 times longer) and in the computer memory requirements (5 times larger). The CPU time for the simulation carried out with the coarsest grid is 20 min while that for the finest grid is 100 min on an IBM SP2 using one processor.

In Section 4, the model is employed to carry out a parametric study on the design and operation of SHESSs for greenhouses. This section has been divided into two parts. First, an infinite array of pipes is considered and the effect of specific parameters on the performance of the system is examined. Next, the parametric study is extended to a full SHESS and its behavior is analysed for different designs.

4. PARAMETRIC STUDY

4.1. *Infinite array of pipes*

The objective here is to examine the effect of key design and operating parameters on the thermal behavior of a SHESS comprising several equally spaced buried pipes. In this case, the system may be seen as an infinite array of pipes and, as a result, the simulations need only to be carried out for a single pipe subjected to the symmetrical boundary conditions shown in Fig. 9. The four parameters considered in this study are the center-to-center distance between the pipes D, their length L, the air velocity inside the pipes V and the moisture content of the soil θ. The range of values used are summarized in Table 2 yielding a total of 240 simulations. The analysis was conducted for a typical soil found below the layer (40 cm) of arable soil in greenhouses and containing few organic matter with a porosity of 0.45. The soil properties were determined with the help of de Vries relations (de Vries, 1975) given by eqns (4) and (5). The constants in these equations were set

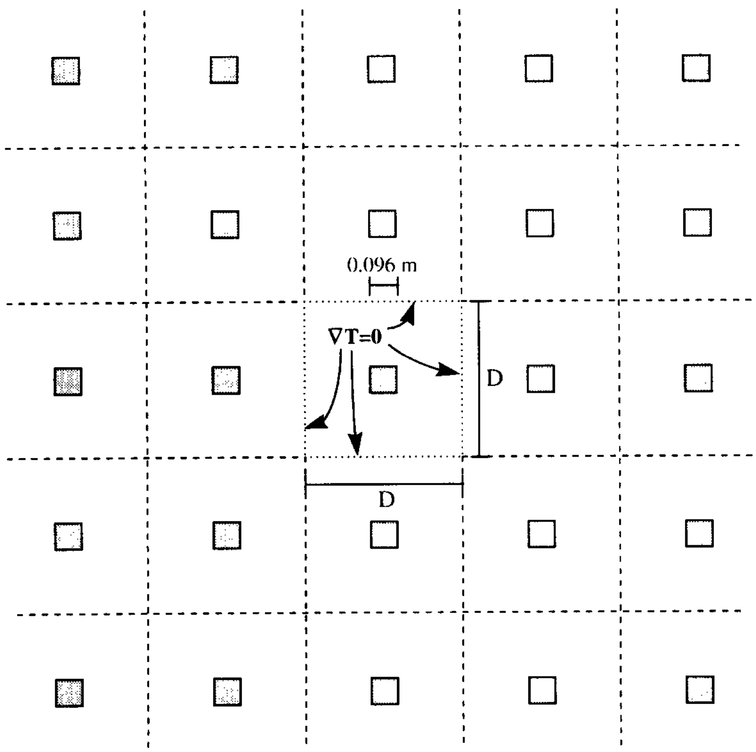

Fig. 9. Schematic representation of an infinite array of pipes in the *xy*-plane.

Table 2. Variable parameters for the infinite array of pipes

θ (m³ of water/m³ of soil)	L (m)	V (m s⁻¹)	D (m)
0.0 ($k=1.2$ W m⁻¹ K⁻¹, $C=1.26$ MJ m⁻³ K⁻¹)	5	2	0.25
0.25 ($k=1.95$ W m⁻¹ K⁻¹, $C=2.31$ MJ m⁻³ K⁻¹)	10	4	0.40
0.45 ($k=2.55$ W m⁻¹ K⁻¹, $C=3.15$ MJ m⁻³ K⁻¹)	20	8	0.55
	30	12	0.70
			0.85

to;

$C_{cte}=1.26\times 106\ \mathrm{Jm^{-3}\,K^{-1}}$

$C_{\theta}=4.2\times 106\ \mathrm{Jm^{-3}\,K^{-1}}$ $k_{cte}=1.2\ \mathrm{Wm^{-1}\,K^{-1}}$

$k_{\theta}=3.0\ \mathrm{Wm^{-1}\,K^{-1}}$

Non-perforated corrugated plastic drainage pipes of 10.8 cm in diameter were retained for the entire study because they are inexpensive and used widely. The pipe inlet air temperature was taken as the experimentally measured temperature for a three day period used for the validation of the model. The inlet absolute humidity was maintained constant at 0.0103 kg water/kg dry air (70% at 20°C). Simulations were performed with grid sizes ranging from $26\times 26\times 15$ to $46\times 46\times 15$ control volumes and timsteps of 300 s. The calculations were pursued for several three-day cycles that is until a cyclic steady-state solution was reached.

Results of the simulations may best be exemplified in terms of the total amount of energy Q_v stored or recovered daily per volume of soil. For example, Fig. 10 displays isocontours of Q_v for a constant moisture content of the soil and two different pipe lengths. Some of the Q_v values are also plotted as a function of the pipe length and of the air velocity in Figs. 11 and 12 respectively. As expected, Q_v decreases exponentially with the pipe center-to-center distance D and length L. The decrease of Q_v with the pipe length is further accentuated as the distance between the pipes becomes smaller (Fig. 11). In contrast, Q_v increases with the air velocity and this effect is enhanced as D diminishes (Fig. 12). Examination of Fig. 10 reveals, however, that a blowing velocity of 4 m s^{-1} is nearly optimal. For $V<4$ m s^{-1}, the total amount of energy stored or recovered drops quickly while for $V>4$ m s^{-1} the gain in Q_v is quickly offset by the substantial increase of the blowing power (the blowing power is proportional to the square of the velocity). Finally, results have shown that as the soil moisture content is augmented, Q_v

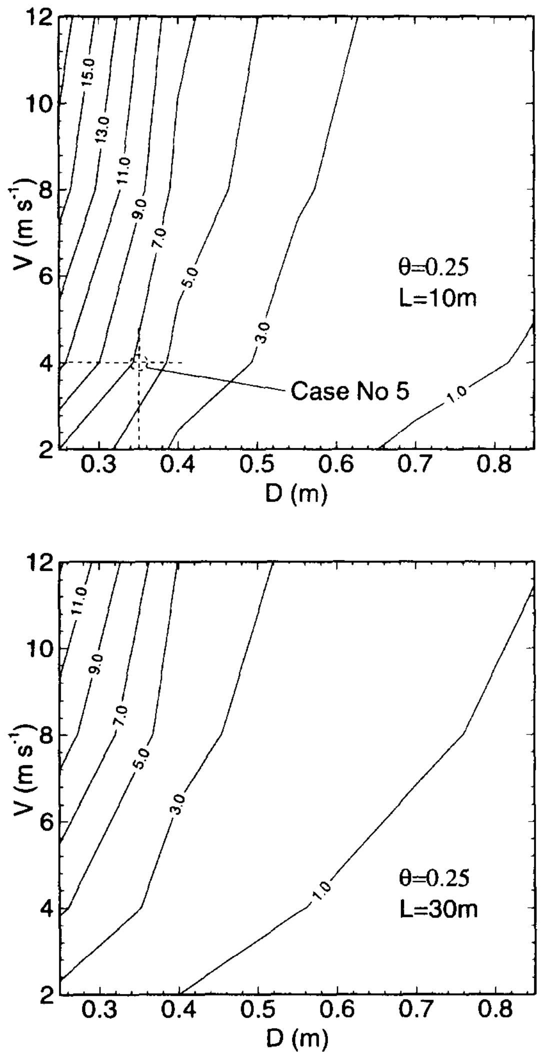

Fig. 10. Storage capacity per unit volume of soil in a day (Q_v) for $\theta = 0.25$.

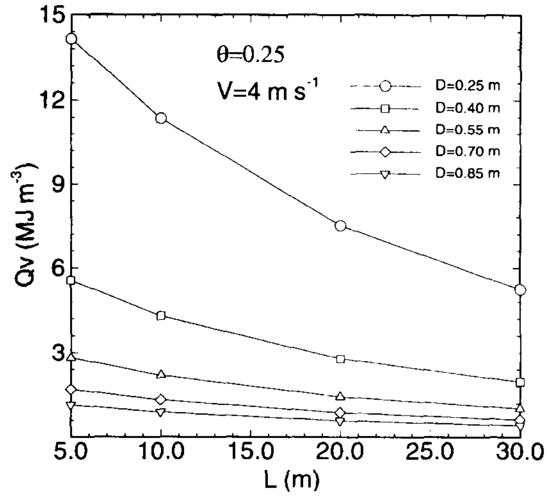

Fig. 11. Storage capacity per unit volume of soil in a day (Q_v) as a function of L for $\theta = 0.25$ and $V = 4\ \mathrm{m\,s^{-1}}$.

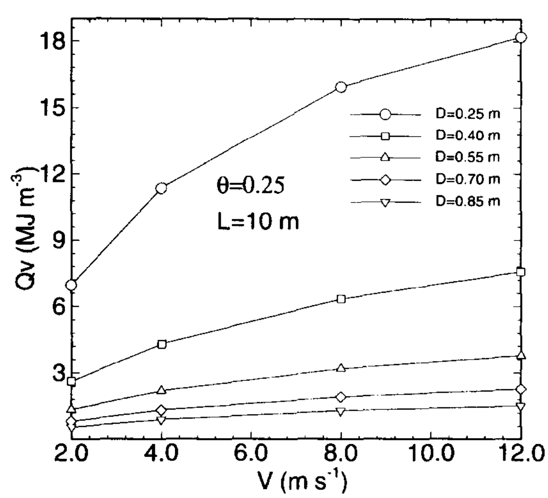

Fig. 12. Storage capacity per unit volume of soil in a day (Q_v) as a function of V for $\theta = 0.25$ and $L = 10$ m.

increases but its effect becomes nearly imperceptible for large L ($L \geq 20$ m) and small V ($\leq 4\ \mathrm{m\,s^{-1}}$).

4.2. Full soil heat exchanger-storage system

Next, the study was extended to a full SHESS. This SHESS was designed with typical values (or nearly optimal values) for D, L and V found in the previous section for an infinite array of pipes. A schematic of the xy-plane of the studied SHESS is provided in Fig. 13 and its main characteristics are summarized in Table 3. The objective here is to determine the effect of the number of pipe rows and their underground depth d, of the foundations and of the insulation on the thermal behavior of the system.

Once again, the non-homogeneous thermophysical properties of the soil were determined using de Vries' relations and are presented in Table 4. The temperatures inside and outside the greenhouse along with the pipe inlet air temperatures and humidities were taken from the experimental measurements used previously. The convective heat transfer coefficient h_c for the air flow inside the corrugated pipes was estimated at $23\ \mathrm{W\,m^{-2}\,K^{-1}}$ using the correlation of Sibley and Raghavan (1984). A heat transfer coefficient of $5\ \mathrm{W\,m^{-2}\,K^{-1}}$ was imposed on the floor inside the greenhouse while a coefficient of $10\ \mathrm{W\,m^{-2}\,K^{-1}}$ was set at the ground surface outside.

Only half of the buried pipes were modelled using a grid of $221 \times 96 \times 10$ non-uniformly distributed control volumes in the x, y and z directions respectively, because of the symmetry

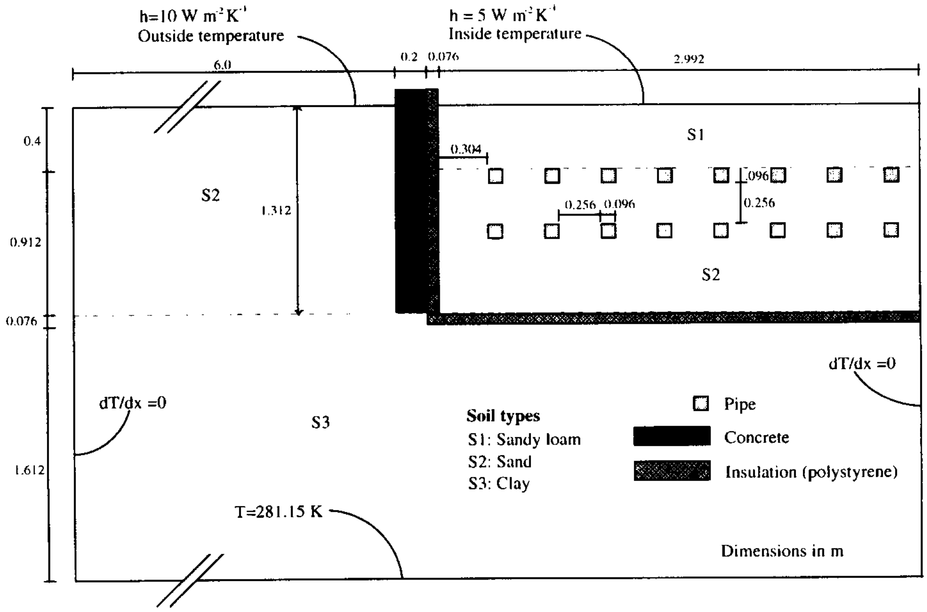

Fig. 13. Schematic representation of the complete SHESS.

Table 3. Characteristics of the full SHESS

Fixed parameters	
Length of the pipes	10 m
Inside width of the greenhouse	6 m
Horizontal distance between pipes	0.352 m (center-to-center)
Vertical distance between pipes	0.352 m (center-to-center)
Constant air velocity in the pipes	4 m s^{-1}
Variable parameters	
Perimeter insulation	0.076 m thick (k=0.027 W m^{-1} K^{-1}; C=6.65 × 10^4 J m^{3-} K^{-1})
Foundation	0.200 m thick × 1.312 m in depth (k=0.72 W m^{-1} K^{-1}; C=1.45 × 10^6 J m^{-3} K^{-1})
Depth of the pipes	0.448 m, 0.608 m, 0.768 m (surface to the center of the upper pipe row)
Insulation under the SHESS	10 × 6 × 0.076 m (located 1.312 m from the ground surface)
Additional row of pipes	0.448 m, 0.800 m, 1.152 m (surface to the center of the first, second and third row)

Table 4. Properties of the soil for the full SHESS

	Porosity	θ	k (W m^{-1} K^{-1})	C (J m^{-3} K^{-1})
Soil type S1	0.6	0.3	1.12	2.08 × 10^6
Soil type S2	0.45	0.25	1.95	2.31 × 10^6
Soil type S3	0.45	0.4	2.4	2.94 × 10^6

of the SHESS layout. To account for the energy drained by the seeping water below the water table, a constant and uniform temperature of 281.15 K was imposed at a depth of 3.0 m below the ground surface. Also, the outermost vertical boundaries of the domain were considered adiabatic.

Ten simulations were carried out with the full SHESS. They are reported in Table 5. Once again, calculations were pursued until a cyclic steady-state solution was reached.

Figure 14 display the isotherm maps at z = 5 m after 2.25 days for cases nos 2, 1 and 7 respectively. In case no. 2 there is no perimeter insulation and a significant fraction of the heat transferred by the SHESS is irremediably wasted to the surrounding soil. Adding perimeter insulation on the foundation of the greenhouse modifies the isotherm maps in the foundation vicinity and reduces the heat losses from the outermost pipes (case no. 1). The heat losses through the horizontal plane underneath the greenhouse do not, however, diminish. To remedy this situation, insulation was also considered under the bottom pipe row (case no. 7). As a result, the temperature of the soil confined by the adiabatic boundaries is much more uniform and, as it will be shown shortly, the performance of the system is greatly enhanced.

The effect of insulating the SHESS on the

Table 5. Simulation and overall performance for the full SHESS

	No of pipe rows	d (m)	Foundation	Insulation (perimeter)	Insulation (under)	Q_s (MJ)	Q_r (MJ)	R Q_r/Q_s
1	2	0.448	yes	yes	no	282.6	208.2	0.737
2	2	0.448	yes	no	no	290.8	197.5	0.679
3	2	0.448	no	yes	no	282.8	207.9	0.735
4	2	0.448	no	no	no	293.6	193.7	0.660
5	2	0.608	yes	yes	no	288.3	205.7	0.714
6	2	0.768	yes	yes	no	292.0	200.0	0.685
7	2	0.448	yes	yes	yes	259.1	239.5	0.924
8	2	0.608	yes	yes	yes	261.2	241.7	0.925
9	2	0.768	yes	yes	yes	263.0	242.8	0.923
10	3	0.448	yes	yes	yes	372.6	353.2	0.948

average pipe outlet air temperature and on the outermost pipe outlet relative humidity is depicted in Figs 15 and 16 respectively. Examination of Fig. 15 reveals that the effect of insulation on the outlet air temperature is nearly inperceptible. The largest temperature differences of the outlet air between cases no. 2 and no. 7 are less than 0.5 K. In contrast, its effect is significant on the relative humidity of the outlet air. Indeed, it is seen that for a well insulated SHESS (case no. 7) condensation in the outermost pipes i.e. the pipes for which this phenomenon is most likely to occur, may be avoided. Consequently, in the early stages of the recovery period at night, no heat will be wasted for evaporating water which accumulates in corrugated pipes of non-insulated SHESS (case no. 2) and the system will immediately deliver sensible heat.

Table 5 also exemplifies, in terms of the recovery ratio R, the overall performance of the SHESS. This ratio is defined as the total amount of energy recovered Q_r over the total amount of energy stored Q_s. The higher this ratio, the better the performance of the SHESS. The quantitites Q_s and Q_r also include the energy transferred through the ground surface which accounts from 10% to 15% of the total energy transferred. In the first four cases, the underground depth d remains constant and equal to 0.448 m and there is no insulation under the bottom pipe row. Results show that the recovery ratio is approximately 73% with insulation around the perimeter of the greenhouse and falls to 67% when the insulation is removed regardless of the foundations. By burying the pipes deeper underground, the situation gets worse (case nos 5 and 6). Indeed, as d increases from 0.448 m to 0.768 m, R decreases from 0.73 to 0.68. For larger depths, more energy is stored during the day but less is recovered at night through the ground surface. On the other hand, adding insulation underneath the bottom pipe row stops heat from leaking to the water table and/or to the surrounding soil which significantly increases the recovery ratio (case nos 7, 8 and 9). In these cases, R remains above 92% and the effect of the depth d is almost imperceptible. Compared to the SHESSs with no underneath insulation (case nos 1–6), the heat losses through the bottom horizontal plane are reduced here by a factor of approximately 4.6! Burying a third row of pipes further enhances the recovery ratio (case no. 10).

5. CONCLUSION

A numerical model for the prediction of the thermal behavior of a SHESS aimed at reducing the energy consumption of greenhouses was developed. The transient fully three-dimensional heat transfer model is based on the coupled conservation equations of energy for the soil and the circulating air. The model takes into account the non-homogeneous properties of the soil and calculates the condensation (heat storage) and evaporation (heat recovery) rates inside the pipes. The model was validated with experimental data taken from a SHESS installed in a commercial type greenhouse. Next, the effect of several design and operating parameters on the heat transfer processes and on the performance of the system were examined. Results have shown that SHESSs are very attractive for reducing the energy consumption of greenhouses as long as they are properly designed and operated. For SHESS involving several buried pipes, it was found that the total amount of energy stored or recovered daily per volume of soil Q_v decreases exponentially with the pipe center-to-center distance and the pipe length. It does however increase with the

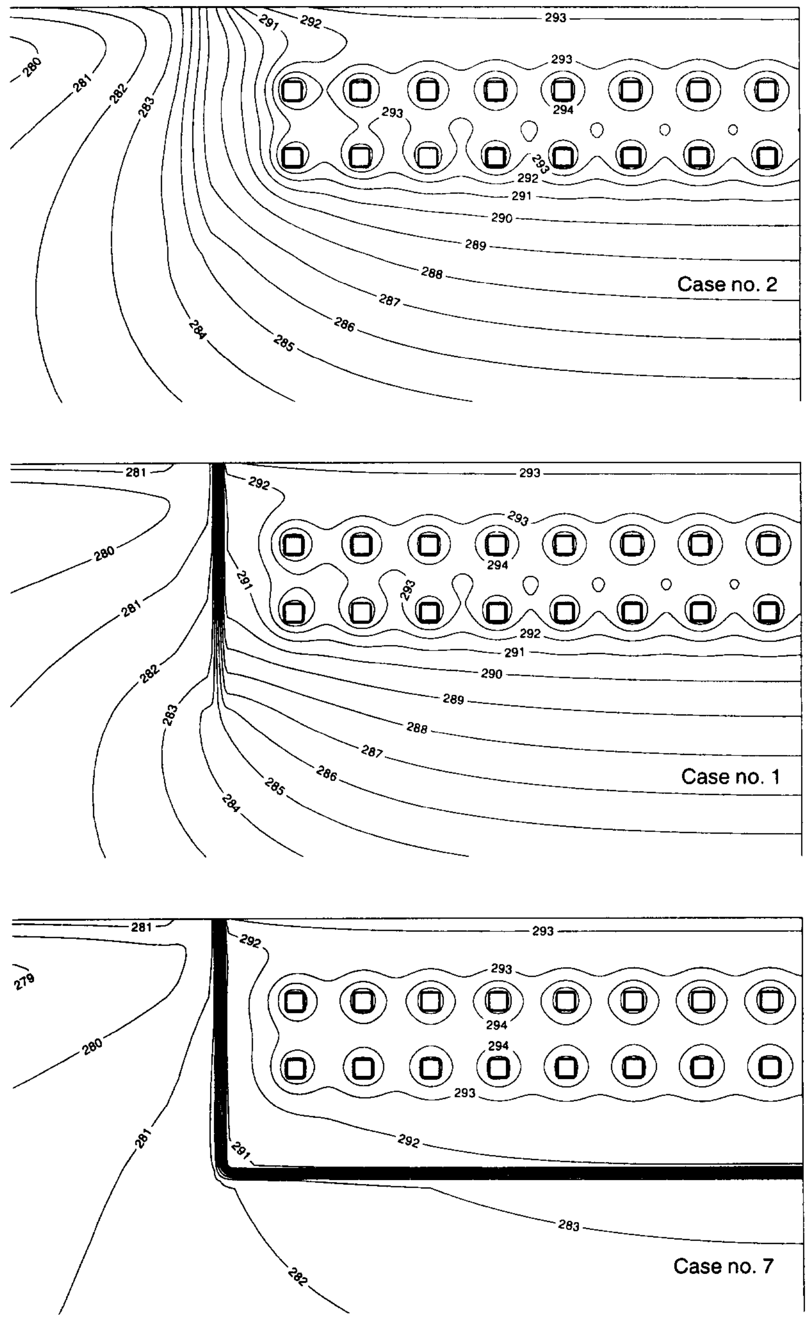

Fig. 14. Isotherm maps for case nos 2, 1 and 7 at $z = 5$ m and $t = 2.25$ days (in Kelvin).

air velocity and this effect is enhanced as the pipe center-to-center distance diminishes. Nevertheless, as a compromise between cost and performance, it was shown that a blowing velocity of $\simeq 4\ \mathrm{m\ s^{-1}}$ is nearly optimal. As the moisture content of the soil increases, Q_v augments but its effect becomes negligible for large pipe lengths and small blowing velocities. The effect of a perimeter foundation on the thermal performance of a SHESS is nearly imperceptible. In contrast, adding perimeter insulation to the SHESS increases the energy recovery ratio R from 67% to 73% and adding bottom insulation further increases it to 92%. Burying pipes deeper underground allows more energy to be stored during the day but less energy is recovered at night through the ground surface and, as a result, the recovery ratio declines.

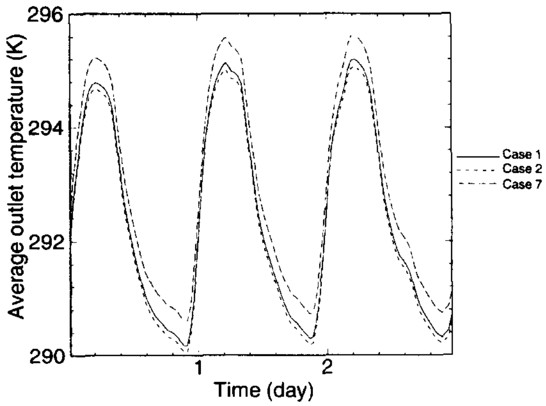

Fig. 15. Time variation of the average pipe outlet temperature for case nos 1, 2 and 7.

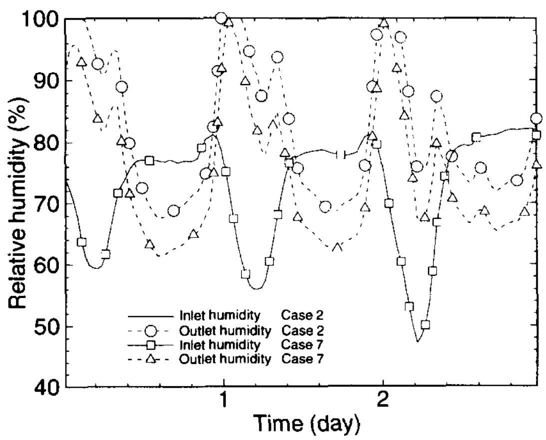

Fig. 16. Time variation of the pipe outlet relative humidity for case nos 2 and 7.

NOMENCLATURE

C Volumetric heat capacity ($J\ m^{-3}\ K^{-1}$)
C_{cte} Volumetric heat capacity of dry soil ($J\ m^{-3}\ K^{-1}$)
C_θ Proportionality constant between the volumetric heat capacity and the soil moisture content ($J\ m^{-3}\ K^{-1}$)
d Distance from the ground surface to the pipe center of the top row (m)
D Center-to-center distance between the pipes (m)
h_c Heat transfer coefficient at the pipe surface ($W\ m^{-2}\ K^{-1}$)
h_L Latent heat of vaporization of water ($\simeq 2.45\ MJ\ kg^{-1}$ between 278 K and 308 K)
H Volumetric enthalpy of moist air ($J\ m^{-3}$)
k Heat conductivity ($W\ m^{-1}\ K^{-1}$)
k_{Cte} Heat conductivity of dry soil ($W\ m^{-1}\ K^{-1}$)
k_θ Proportionality constant between the heat conductivity and the soil moisture content ($W\ m^{-1}\ K^{-1}$)
L Length of the pipes (m)
P Perimeter of a pipe cross-section (m)
q Heat entering the pipe per unit length ($W\ m^{-1}$)
q_P Heat entering the pipe control volume P (W)
Q_r Total amount of energy recovered during one night (J)
Q_s Total amount of energy stored during one day (J)
Q_v Total amount of energy stored or recovered daily per volume of soil ($J\ m^{-3}$)
R Ratio of the amount of energy stored during the day over the amount of energy recovered during the night (Q_s/Q_r)
S Source term ($W\ m^{-3}$)
S_C Constant part of the source term ($S=S_c+S_t^*T$) ($W\ m^{-3}$)
SHESS Soil Heat Exchanger-Storage System
S_t Temperature dependencies of the source term ($S=S_c+S_t^*T$) ($W\ m^{-3}\ K^{-1}$)
t Time (s)
T Temperature within the soil (K)
T_{air} Air temperature inside the pipe (K)
T_P^0 Temperature at the center of the control volume P at the previous time step
T_{soil} Temperature at the pipe surface (K)
V Air flow velocity ($m\ s^{-1}$)
x, y, z Space coordinates (m)

Greek

δt Time step (s)
δV_P Volume of the control volume P (m^3)
δx_P, δy_P, δz_P x, y and z dimensions of the control volume P (m)
θ Volumetric soil moisture content (m^3 of water/m^3 of soil)
ρ Density of dry air ($kg\ m^{-3}$)
ω Absolute air humidity (kg of water vapor/kg of dry air)
ω

Subscripts

P Node at the center of a control volume
W, E, S, N, B, T West, east, south, north, bottom and top nodes

Acknowledgements—The authors are grateful to the Ministère des ressources naturelles du Québec for the financial support of this project.

REFERENCES

AEA Industrial Technology (1992), FLOW3D, Release 3.2: User Manual. Harwell Laboratory, Oxfordshire, UK.
Bernier H., Raghavan G.S.V. and Paris J. (1990a) *Evaluation of a Soil Heat Exchanger-Storage System for a Greenhouse. Part I: System Performance.* Canadian Agricultural Engineering, Vol. 33, 093–098.
Bernier H., Raghavan G.S.V. and Paris J. (1990b) *Evaluation of a Soil Heat Exchanger-Storage System for a Greenhouse. Part II: Energy Saving Aspects*, Canadian Agricultural Engineering, Vol. 33, 099–105.
de Vries D.A. (1975) Transfer process in plant environment. In *Heat Transfer in Soil, Heat and Mass Transfer in the Biosphere*, D.A. de Vries and N.H. Afgan (Eds) Vol. 1, Script a Book Company.
Gauthier C. (1994) Transfert de chaleur et d'humidité dans le sol. Internal report, Groupe de recherche THERMAUS. Département de génie mécanique, Université de Sherbrooke.
Mihalakakou G., Santamouris M. and Asimakopoulos D. (1994a) Modelling the thermal performance of earth-to-air heat exchangers. *J. Solar Energy* **53**, 301–305.
Mihalakakou G., Santamouris M. and Asimakopoulos D. (1994b) Use of the ground for heat dissipation. *Energy* **19**, 17–25.
Mihalakakou G., Santamouris M., Asimakopoulos D. and Argiriou A. (1995) On the ground temperature below buildings. *J. Solar Energy* **55**, 355–362.

Puri V.M. (1986) Feasibility and performance curves for intermittent earth tube heat exchangers. *Am. Soc. Agricul. Eng.* **29**, 526–532.

Rodriguez E.A., Cjudo J.M. and Alvarez S. (1988) Earth-tube systems performance. In *Proc. CIB Meet., Air Quality and Air Conditioning.* Paris, France.

Santamouris M. and Lefas C.C. (1986) Thermal analysis and computer control of hybric greenhouse with subsurface heat storage. *Energy Agriculture* **5**, 161–173.

Santamouris M., Balaras C.A., Dascalaki E. and Vaillindras M. (1994) Passive solar agricultural greenhouses: a worldwide classification and evaluation of technologies and systems used for heating purposes. *J. Solar Energy* **53**, 411–426.

Sawhney R.L. and Mahajan U. (1994) Heating and cooling potential of an underground air-pipe system. *Int. J. Energy Res.* **18**, 509–524.

Schiller G. (1982) Earth tubes for passive cooling. The development of a transient numerical model for predicting the performance of earth/air heat exchangers. Project Report for MS degree, MIT, Mechanical Engineering.

Sibley K.J. and Raghavan G.S.V. (1984) Heat transfer coefficients for air flow in plastic corrugated drainage tubes. *Canadian Agricultural Engineering* **26**, 177–180.

Sodha M.S., Mahajan U. and Sawhney R.L. (1994) Thermal performance of paallel earth air-pipes system. *Int. J. Energy Res.* **18**, 437–447.

Tzaferis A., Liparakis D., Santamouris M. and Argiriou A. (1992) Analysis of the accuracy and sensitivity of eight models to predict the performance of earth-to-air heat exchangers. *Energy and Buildings* **18**, 35–43.